Bivalent Ligands with Long Nanometer-Scale Flexible Linkers[†]

Ling Tian and Tomasz Heyduk*

Edward A. Doisy Department of Biochemistry and Molecular Biology, St. Louis University Medical School, 1100 South Grand Boulevard, St. Louis, Missouri 63104

Received August 27, 2008; Revised Manuscript Received November 15, 2008

ABSTRACT: High-affinity ligands recognizing biomolecules with high specificity are crucial for drug discovery and biomolecule detection. We describe here a simple approach to preparing aptamer-based ligands with enhanced binding affinity. In this approach, two aptamer ligands with suboptimal binding properties are covalently linked with a long flexible linker to create a bivalent ligand with significantly improved binding affinity. We first used a simple oligonucleotide-based model, which mimicked the interaction between bivalent ligands and their target molecules, to investigate the principles governing the affinity enhancement. These experiments showed that as long as the individual ligands had at least submicromolar binding affinities, they could be linked with a nanometer-scale flexible linker to produce bivalent ligands with improved binding affinity and specificity. Furthermore, comparison of the experimental data with the bivalent ligand properties predicted by a wormlike chain model showed that this model provided a good approximation of the binding properties of nanometer-scale flexible bivalent ligands. To verify the practicality of bivalent ligands with nanometer-scale flexible linkers, we constructed aptamer-based bivalent ligands for human α-thrombin. In agreement with the predictions derived from the model system, the binding affinities and the anticlotting activities of thrombin bivalent ligands were significantly improved compared to those of the individual ligands.

High-affinity specific ligands for various biological targets are highly desired for sensitive detection of biomolecules and for therapeutic applications. Typically, such ligands are polyclonal or monoclonal antibodies or antibody fragments. More recently, recombinant antibodies and antibodies derived from in vitro selection approaches became available as a new source of useful ligands (*1, 2*). The most recent addition to the repertoire of affinity ligands includes constructs derived from alternative protein scaffolds (for example, affibodies based on a small triple-helical motif derived from *Staphylococcus* protein A) (*3*). Finally, a discovery made in 1990 revealed a potential for using nucleic acids as building materials for ligands capable of binding biological targets with affinities and specificities approaching those observed for antibodies (*4, 5*).

Nucleic acid-based ligands (aptamers) are obtained by an in vitro selection procedure (SELEX)[1] that allows one to select aptamers starting from a highly complex library of random sequence oligonucleotides (*4, 5*). Aptamers are very attractive ligands for therapeutic or diagnostic applications since they can be synthesized chemically, allowing for facile replication in large quantities. They can be easily chemically modified for conjugation to other molecules, particles, or solid supports. They also exhibit low immunogenicity (*6*−*8*). Aptamers with reasonable binding affinity for a large number of various biological targets have been developed, and for a much smaller number of targets, aptamers with affinities and specificities rivaling antibodies have been obtained. Procedures which would allow improvements in affinity and specificity of aptamer-based ligands would be very desirable as they will permit more efficient utilization of the relative ease in developing the aptamers, many of which have suboptimal binding properties.

Bi- or multivalency is often used in nature to increase affinity and/or specificity of macromolecular interactions. One potentially simple approach to improving the properties of the ligands would be thus to construct a multivalent ligand by connecting ligands binding the target at nonoverlapping sites. A number of bivalent ligands have been developed and shown to improve the potency, selectivity, intrinsic activity, and in vivo profile of the corresponding monomer (for example, refs *9*− *14*). Design of multivalent ligands is often challenging since the rules of additivity of binding free energies for such ligands are complicated (*15*). The behavior of bivalent ligands connected by peptide linkers has been successfully analyzed by theory, and the conclusions of this analysis were verified experimentally (*16, 17*).

Aptamers are particularly attractive blocks for building multivalent ligands since they can be synthesized in a straightforward manner and covalently linked using well-established methodologies. The great potential of multivalent aptamer constructs has been already demonstrated (*18*−*20*). The goal of this work was to develop a simple approach to creating improved aptamer-based ligands via covalent linking of a very long PEG-based flexible linker with the two aptamers binding to the nonoverlapping sites on the target. One of the challenges in creating effective bivalent ligands

[†] This work was supported by American Heart Association Grant 0750027Z.

* To whom correspondence should be addressed. E-mail: heydukt@slu.edu. Fax: (314) 977-9205. Phone: (314) 977-9238.

[1] Abbreviations: SELEX, systematic evolution of ligands by exponential enrichment; aPPT, activated partial thromboplastin time; FL, fluorescein.

10.1021/bi801630b CCC: $40.75
Published on Web 12/29/2008

Table 1: Oligonucleotide Constructs for Studies with Model Bivalent Ligands[a]

Name	Sequence
A	dabcyl-TCTGCGAC
B	CTGGACGT-dabcyl
A(24nm)B	dabcyl-TCTGCGAC(Spacer18)$_{10}$CTGGACGT-dabcyl
A(36nm)B	dabcyl-TCTGCGAC(Spacer18)$_{15}$CTGGACGT-dabcyl
A(48nm)B	dabcyl-TCTGCGAC(Spacer18)$_{20}$CTGGACGT-dabcyl
T(6nm)0	Cy5-TCGCTAGCGTGCTGCCGT-FL CGGTGACCTGCATAGCGATCGCACGACGGCATAGACGCTGAGCC
T(6nm)1	Cy5-TCGCTAGCGTGCTGCCGT-FL CGGTGACCTGCATAGCGATCGCACGACGGCATAGACGC**A**GAGCC
T(6nm)2	Cy5-TCGCTAGCGTGCTGCCGT-FL CGGTG**T**CCTGCATAGCGATCGCACGACGGCATAGACGCTGAGCC
T(6nm)3	Cy5-TCGCTAGCGTGCTGCCGT-FL CGGTG**T**CCTGCATAGCGATCGCACGACGGCATAGACGC**A**GAGCC
T(6nm)4	Cy5-TCGCTAGCGTGCTGCCGT-FL CGGTGACC**G**GCATAGCGATCGCACGACGGCATAG**G**CGCTGAGCC
T(9nm)0	Cy5-TCGCTAGCGAGTAGGCGTATGCTGCCGT-FL CGGTGACCTGCATAGCGATCGCTCATCCGCATACGACGGCATAGACGCTGAGCC
T(9nm)4	Cy5-TCGCTAGCGAGTAGGCGTATGCTGCCGT-FL CGGTGACC**G**GCATAGCGATCGCTCATCCGCATACGACGGCATAG**G**CGCTGAGCC
T(13nm)0	Cy5-TCGCTAGCGAGTAGCTCGATGCTAGCGTATGCTGCCGT-FL CGGTGACCTGCATAGCGATCGCTCATCGAGCTACGATCGCATACGACGGCATAGACGCTGAGCC
T(13nm)4	Cy5-TCGCTAGCGAGTAGCTCGATGCTAGCGTATGCTGCCGT-FL CGGTGACC**G**GCATAGCGATCGCTCATCGAGCTACGATCGCATACGACGGCATAG**G**CGCTGAGCC

[a] Bold and underlined bases depict base changes made to the target construct to modulate the intrinsic affinity of the ligand components of bivalent ligands.

is ensuring that the overall conformation of the bivalent ligand would allow simultaneous binding interactions of the two aptamers without free energy losses due to steric hindrance or incorrect spacing and/or orientation of the aptamers. We hypothesized that the use of a long flexible linker will eliminate this challenge and will allow a practical compromise between the ease of the preparation of such bivalent ligands and the degree to which their binding properties are improved. Our previous work with aptamer-based sensors employing long flexible linkers (*21*) provided additional support for this hypothesis. Additionally, long flexible linkers should allow us to design ligands binding large targets since they will allow the two aptamers to bind to the sites separated by large distances. We have first used a simple model system to characterize the binding properties of such bivalent ligands. We have then applied these concepts to design bivalent ligands targeting thrombin. In agreement with the expectation derived from the analysis of the model system, bivalent ligands targeting thrombin exhibited markedly improved binding affinities and anticlotting activities compared to the corresponding monomers. Our simple strategy for designing improved ligands is not limited to aptamer-based ligands and can be applied more generally to create bivalent ligands using other affinity ligands (for example, antibodies or antibody fragments). A preliminary account of this work was presented elsewhere (*22*).

MATERIALS AND METHODS

Materials. Oligonucleotide constructs used throughout this study are listed in Tables 1 and 2. Oligonucleotides were obtained from Keck Oligonucleotide Synthesis Facility at Yale University or from IDT (Coralville, IA). 3′-Fluorescein and 5′- or 3′-dabcyl were incorporated into oligonucleotides using appropriate phosphoramidates during oligonucleotide synthesis. 5′-Cy5 was incorporated into oligonucleotides by postsynthetic modification with Cy5-NHS of oligonucleotides containing C6 amino-dT at the 5′-end (Amersharm Biosciences, Piscataway, NJ). Flexible linkers of variable length were added to the oligonucleotide constructs by incorporating various amounts of Spacer18 phosphoramidate. The length of one Spacer18 unit [5′-$(OCH_2CH_2)_6$-OPO_3-3′] is ~2.4 nm. All modified oligonucleotides were purified by reversed-phase HPLC, while unmodified oligonucleotides were purified by electrophoresis on a 12% polyacrylamide−urea gel. Concentrations of all oligonucleotides were calculated from the UV absorbance at 260 nm after correction for the contribution of the fluorophore absorbance at 260 nm. To obtain the target (T in Figure 1B), equimolar amounts of appropriate complementary oligonucleotides were mixed at a concentration of 10 μM in 100 μL of binding buffer, heated for 1 min at 95 °C, and cooled to 25 °C over 1 h. Biv peptide was synthesized by the Keck Oligonucleotide Synthesis Facility at Yale University. Human normal pooled plasma was from George King Biomedical, Inc. (Overland Park, KS). aPTT reagent ALEXIN was from Trinity Biotech USA (St. Louis, MO). Human α-thrombin was a generous gift from A. Rezaie (St. Louis University).

Conjugation of biv [a variant of bivalirudin, a synthetic peptide that directly inhibits thrombin by specifically binding to the catalytic site as well as to the anion-binding exosite,

Table 2: Constructs for Studies with Bivalent Thrombin Ligands

Name	Sequence
A1	AGTCCGTGGTAGGGCAGGTTGGGGTGACT
A2	GGTTGGTGTGGTTGG
A1FL	FL-AGTCCGTGGTAGGGCAGGTTGGGGTGACT
A2FL	FL-GGTTGGTGTGGTTGG
A1(12nm)A2	AGTCCGTGGTAGGGCAGGTTGGGGTGACT(Spacer18)$_5$GGTTGGTGTGGTTGG
A1(24nm)A2	AGTCCGTGGTAGGGCAGGTTGGGGTGACT(Spacer18)$_{10}$GGTTGGTGTGGTTGG
A2(24nm)A1	GGTTGGTGTGGTTGG(Spacer18)$_{10}$AGTCCGTGGTAGGGCAGGTTGGGGTGACT
BC1	FL-AGATGCG(Spacer18)$_5$AGTCCGTGGTAGGGCAGGTTGGGGTGACT
BC2	GGTTGGTGTGGTTGG(Spacer18)$_5$-Cy5-CGCATCT
anti-A1	AGTCACCCCAACCTGCCCTACCACGGACT
anti-A2	CCAACCACACCA
biv	(D-Phe)-Pro-Arg-Pro-Gly-Gly-Cys-Gly-Asn-Gly-Asp-Phe-Glu-Ile-Pro-Glu-Glu-Tyr-Leu
biv (24nm)A1	Biv(spacer18)$_{10}$AGTCCGTGGTAGGGCAGGTTGGGGTGACT

in which a glycine residue at position 7 was replaced with cysteine (Table 2)] with A1 aptamer to yield the biv(24nm)A1 construct (Table 2) was accomplished by cross-linking biv peptide with 5′-amino-C6-(spacer18)$_{10}$-AGT CCG TGG TAG GGC AGG TTG GGG TGA CT-3′ (corresponding to the A1 aptamer sequence with a PEG-based linker plus a 5′-amino C6 added to the 5′-end) using SMCC [sulfosuccinimidyl 4-(*N*-maleimidomethyl)cyclohexane-1-carboxylate] (Pierce, Rockford, IL). The oligonucleotide and SMCC (predissolved in DMF) were first incubated in 0.1 M $NaHCO_3$ buffer (pH 7.35) for 3 h at room temperature at a molar ratio of 1:25. Excess SMCC was removed by ethanol precipitation. The biv peptide was treated with 5 mM TCEP [tris(2-carboxyethyl)phosphine] (Pierce) at room temperature for 30 min and then mixed with the ethanol-precipitated oligonucleotide−SMCC conjugate at a molar ratio of 20:1 in 0.1 M $NaHCO_3$ buffer (pH 7.35). Reaction was carried out at room temperature for at least 6 h. Biv(24nm)A1 was purified by reverse-phase HPLC or by native PAGE.

Binding Measurements. Binding of bivalent ligands to the target was quantified by measuring fluorescence quenching of fluorescein or Cy5 dyes incorporated into the target by dabcyl quenchers attached to the ends of the ligand. Fluorescence was read with a Fluorolog-3 spectrofluorometer or a MicroMax 384 Microwell plate reader (Jobin Yvon Inc., Edison, NJ). The intensity of fluorescein emission at 520 nm was measured with excitation at 485 nm, and Cy5 emission at 666 nm was read with excitation at 643 nm. Reaction mixtures were prepared in binding buffer [50 mM Tris-HCl (pH 7.5), 5 mM KCl, 100 mM NaCl, 1 mM $MgCl_2$, and 0.1 mg/mL BSA], and the fluorescence intensity was read after incubation for 40 min at 25 °C. An appropriate incubation time (40 min) was established by kinetic experiments in which the binding was monitored as a function of time.

Binding of A1 aptamer (Table 2) to thrombin was assessed by fluorescence polarization. An 8 nM solution of fluorescein-labeled A1 [A1FL (Table 2)] was titrated with thrombin in 120 μL of binding buffer at 25 °C. The fluorescence anisotropy was measured after incubation for 40 min using a Fluorolog-3 spectrofluorometer.

Binding of A2 (Table 2) to thrombin was assessed by thrombin-dependent quenching of fluorescence of fluorescein-labeled A2 [A2FL (Table 2)]. A2FL (10 nM) was titrated with thrombin in 20 μL of binding buffer. Fluorescein emission was measured in 384-well microplates after incubation for 40 min at 25 °C with a Tecan (Research Triangle Park, NC) SpectraFluorPlus microplate reader. The binding affinity of bivalirudin and A1(12nm)A2 for thrombin was measured by the assay described above for A2FL in a competition assay format. A mixture of 10 nM A2FL and 15 nM thrombin was titrated with bivalirudin or A1(12nm)A2 in 20 μL of binding buffer. Reaction mixtures were incubated at 25 °C for 40 min, and fluorescein emission was measured in 384-well microplates using a SpectraFluorPlus microplate reader.

The binding affinity of A1(24nm)A2 and A2(24nm)A1 was too high to be measured by a competition assay involving A2FL and thrombin described above. To assess the relative binding affinity of these ligands, we used a competition assay employing molecular beacons for thrombin (*21*). Interaction between thrombin and its molecular beacon is much stronger compared to the binding of A2FL to thrombin, allowing more precise evaluation of the affinity

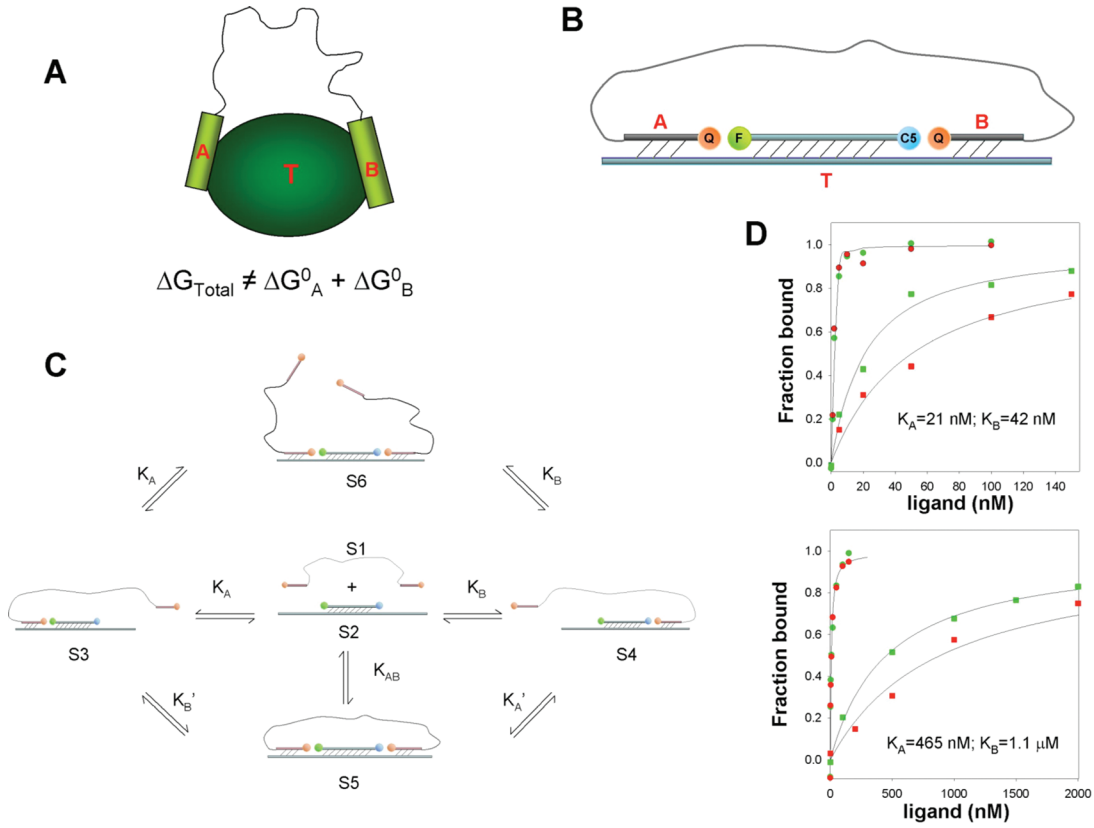

FIGURE 1: (A) Schematic representation of a complex between a target and a bivalent ligand composed of two ligands ("A" and "B") connected by a long flexible linker. The expression for a total free energy change upon complex formation is shown as well (the meaning of the individual terms is discussed in the text). (B) Oligonucleotide-based model for studying the relationship among the affinity of individual ligands, the length of the flexible linker, the distance between the binding sites, and the overall binding affinity of the bivalent ligand. (C) Binding equilibria of the oligonucleotide-based model. (D) Examples of the effect of linking two individual ligands with a flexible linker on binding affinity. Green squares denote binding of individual ligand A (Table 1); red squares denote binding of individual ligand B (Table 1), and green and red circles denote binding of bivalent ligand A(24nm)B (Table 1) monitored by fluorescein and the Cy5 fluorescence signal, respectively. Top and bottom panels depict the binding to T(6nm)0 and T(6nm)3 targets (Table 1), respectively. Solid lines depict the best fit of the data to the model depicted in panel C.

of tight binding ligands competing with the molecular beacon. However, the stability of a complex between thrombin and a molecular beacon is a more complex function of at least three molecular contacts, making direct determination of the binding constants for the competing ligands difficult. We used thus a thrombin molecular beacon competition assay only to determine the relative affinity of A1(12nm)A2, A1(24nm)A2, and A2(24nm)A1. We then used this information to calculate the dissociation constants for for dissociation of A1(24nm)A2 and A2(24nm)A1 from the dissociation constant for A1(12nm)A2 that was determined using a simple competition assay employing A2FL and thrombin. The thrombin beacon competition assay was performed in 384-well plates in 20 μL of binding buffer volume. A mixture of 100 nM BC1 and BC2 (Table 2) and 40 nM thrombin was titrated with corresponding thrombin ligands. After incubation for 40 min at 25 °C, the FRET signal of the thrombin beacon (*21*) was read with a SpectraFluorPlus microplate reader.

Analysis of Binding Data. All binding data were analyzed by numerical nonlinear regression fitting with Scientist (MicroMath, Salt Lake City, UT). Titrations of model targets with model bivalent ligands when fluorescein quenching was used as a signal were fitted to

$$F = F_{free}([S2] + [S4]) + F_{bound}([S3] + [S5] + [S6]) \quad (1)$$

where F is the observed fluorescence intensity, F_{free} is the unquenched specific fluorescence intensity, and F_{bound} is the quenched specific fluorescence intensity. S1−S6 correspond to the species depicted in Figure 1C. Titrations of model targets with model bivalent ligands when Cy5 quenching was used as a signal were fitted to

$$F = F_{free}([S2] + [S3]) + F_{bound}([S4] + [S5] + [S6]) \quad (2)$$

Titrations of A1FL with thrombin using fluorescence polarization as an observable and the competition variant of the assay were fitted to

$$pol = pol_{free}[A1FL_{free}] + pol_{bound}[A1FL{-}thrombin] \quad (3)$$

where pol is the observed fluorescence polarization and pol_{free} and pol_{bound} are the specific fluorescence polarizations of free A1FL and A1FL bound to thrombin, respectively.

Titrations of A2FL with thrombin using fluorescence quenching as observable, and the competition variants of the assay were fitted to

$$F = F_{free}[A2FL_{free}] + F_{bound}[A2FL{-}thrombin] \quad (4)$$

where F is the observed fluorescence intensity and F_{free} and F_{bound} are specific fluorescence intensities of free A2FL and A2FL bound to thrombin, respectively.

During the fitting, concentrations of all species in eqs 1−4 were calculated numerically for each point by solving the appropriate set of mass conservation equations defined by the particular model (for example, a model illustrated in Figure 1C in the case of eqs 1 and 2).

Thrombin Clotting Assay. Activated partial thromboplastin time (aPTT) (*23*) was measured with ST4 Biocoagulometer (Diagnostica/Stago, Asnieres, France). Reaction mixtures contained 50 μL of human normal plasma {1:4 dilution in TE buffer [20 mM Tris (pH 7.4) and 100 mM NaCl]} and 50 μL of ALEXIN reagent (purified rabbit brain cephalin in ellagic acid, 0.1 mM; 1:4 dilution in TE buffer) with and without the corresponding thrombin ligands (final concentration of 200 nM, in TE buffer). Reaction mixtures were incubated at 37 °C for 5 min, and clotting was initiated by the addition of 50 μL of 35 mM $CaCl_2$.

RESULTS

Oligonucleotide-Based Model for Analyzing Bivalent Ligand Properties. Figure 1A schematically depicts a bivalent ligand containing two independent binders (A and B) connected by a long flexible linker. The rules of free energy additivity in bivalent ligands were analyzed by Jencks (*15*). The free energy of the association of a bivalent ligand with the target (T) is not a simple summation of binding free energies for the individual ligand components of the bivalent ligand. There are various entropic and enthalpic consequences of linking the two ligands that are generally difficult to estimate. Thus, in general, predicting the affinity of the bivalent ligand based on known individual affinities for the ligand components of the bivalent ligand is at best difficult.

The effect of the linker can be described using a simple formalism of effective concentration (c_{eff}) (*16, 17*):

$$c_{eff} = K_A K_B / K_{AB} \quad (5)$$

where K_A and K_B are dissociation constants of the individual ligands and K_{AB} is a dissociation constant of the bivalent ligand. Theoretical calculations of c_{eff} have been attempted. Crothers and Metzger used particle-in-a-sphere approximation (*24*) to estimate c_{eff}. Zhou developed a more realistic wormlike chain model that provided a good approximation of the behavior of semiflexible polypeptide-based linkers (*16, 17*). Rather than using theoretical predictions for c_{eff}, we have designed a simple oligonucleotide-based model (Figure 1B) that allowed experimental determinations of c_{eff} values for the nanometer-scale flexible linkers used in our project.

Figure 1B illustrates the design of the model system that we have implemented for the analysis of the properties of bivalent ligands containing long flexible linkers. The "ligands" were prepared by linking two single-stranded oligonucleotides with PEG-based flexible linkers. The model "target" was a DNA duplex with single-stranded extensions containing sequences complementary to the oligonucleotides of the ligand. We have introduced fluorescence probes (fluorescein and Cy5, respectively) to the target construct in the vicinity of single-stranded extensions (Figure 1). The ligands had quencher probes (dabcyl) incorporated into the ends of the oligonucleotides. When the ligand binds to the target, the quencher is placed in the proximity of the corresponding fluorescence probe, resulting in a quenching of the fluorescence signal of the probe. Observing changes in the fluorescence emission of fluorescein and Cy5 allowed independent monitoring of binding of each of the "halves" of the bivalent ligand. This model system allowed convenient analysis of the effect of linker length, the distance between the binding site of the target, and the affinity of the individual components of the bivalent ligand on the overall affinity of the bivalent ligand.

Figure 1C depicts various possible complexes (S3−S6) that can form from free ligand (S1) and free target (S2). Equilibria depicted in Figure 1C do not include all possible complexes that in principle could form. For example, higher-order complexes (containing more then one molecule of the target) could form by association of another target molecule with S6, S4, or S3. However, such complexes are very unlikely to be present in significant amounts under experimental conditions used in our experiments, and they were ignored in our model used for the analysis. This has been verified by computer simulations of relative amounts of such higher-order complexes performed assuming a wide range of equilibrium constants for the equilibria depicted in Figure 1C (Table S2 of the Supporting Information).

Equilibria depicted in Figure 1C can be described using a set of four equilibrium constants (K_A, K'_A, K_B, and K'_B), three of which are independent since

$$K_A K'_A = K_B K'_B \quad (6)$$

where K_A and K_B are dissociation constants of the individual ligands whereas K'_A and K'_B are isomerization constants that describe the relative stability of the complex between the bivalent construct and the target in which both component ligands are associated with their binding sites compared to the complex in which only one of the ligands is associated with its binding site (Figure 1C). The simplest formalism for quantitatively evaluating the effect of the flexible linker on the binding affinity of bivalent constructs is to use the value of a parameter c_{eff} that can be calculated from eq 5. c_{eff} is given in units of concentration and can be considered to be the effective relative local concentration of ligands resulting from their attachment by a flexible linker.

Figure 1D shows examples of a couple of typical results of the titration of the target with the ligands. This figure shows comparisons of titrations with individual ligands with titrations with corresponding bivalent ligands. Greatly enhanced affinity of bivalent ligands is obvious. Solid lines represent the best fit of the binding data to a model describing a simple binding process (in the case of the individual ligand) or a binding process considering all the species illustrated in Figure 1C (in the case of the bivalent ligand). When the data obtained with bivalent ligands were fit, the dissociation constants (K_A and K_B) describing the interactions of the individual components of the bivalent ligand were fixed at the values obtained from the analysis of binding data for the individual ligands. This was justified by a lack of cooperativity of the binding of individual ligands. In control experiments, we did not observe a significant difference in the binding affinity of the individual ligand when it was determined in the absence or presence of a saturating concentration of the other individual ligand (data not shown).

To characterize the binding properties of bivalent ligands, we prepared a series of bivalent ligand constructs and the corresponding targets (Table 1). The three ligands contained flexible linkers of varying length (24, 36, and 48 nm). The

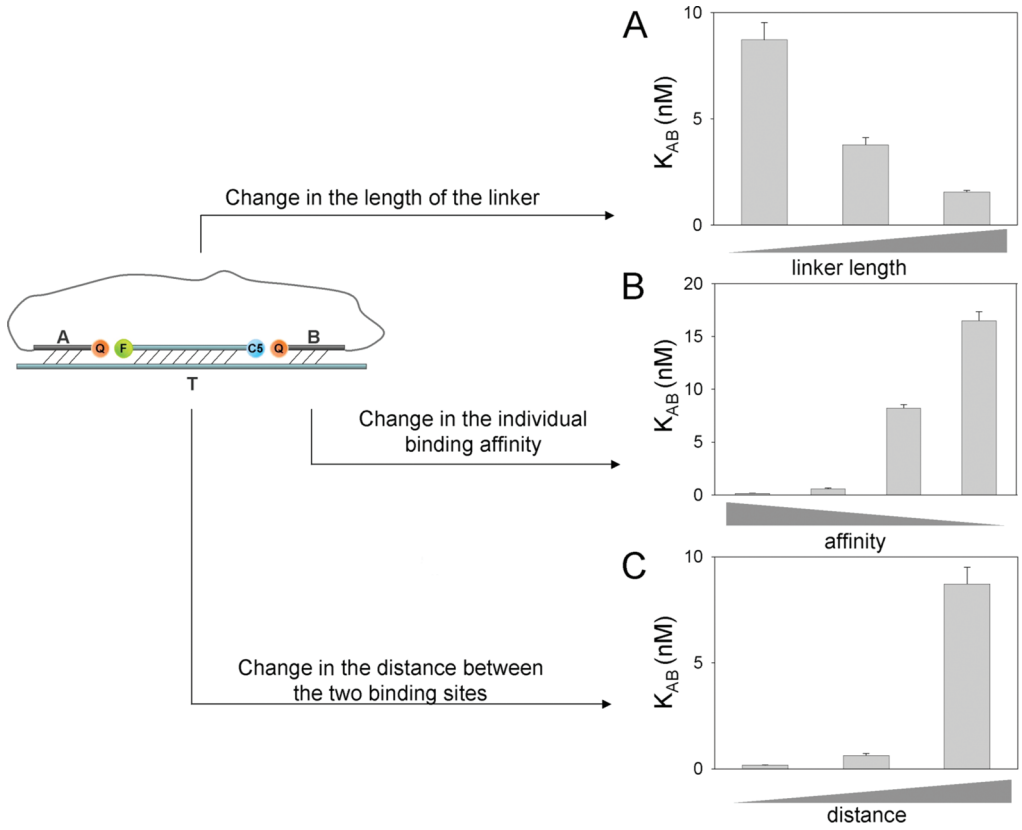

FIGURE 2: Examples of the effects of the changes in the length of the linker (A), the affinity of the individual ligands (B), and the distance between the binding sites (C) on the affinity (dissociation constant) of the bivalent ligand. The data shown in panel A correspond to target T(13nm)0 (Table 1) titrated with ligands A(24nm)B, A(36nm)B, and A(48nm)B (Table 1). The data shown in panel B correspond to targets T(6nm)0, T(6nm)2, T(6nm)3, and T(6nm)4 (Table 1) titrated with ligand A(24nm)B (Table 1). The data shown in panel C correspond to targets T(6nm)0, T(9nm)0, and T(13nm)0 (Table 1) titrated with ligand A(24nm)B (Table 1). Dissociation constants (K_A and K_B) for the individual ligands for the bivalent ligands in panels A and C were 21 and 42 nM, respectively. In panel B, these values were (for each of the bars shown, from left to right) 21 and 42 nM, 17 and 828 nM, 465 and 1100 nM, and 1000 and 1700 nM.

nine target constructs contained various combinations of three distances between the ligand binding sites (6, 9, and 13 nm) and ligand binding sites of various intrinsic binding affinities. We used these constructs to determine the effects of ligand linker length, the distance between the binding sites of the target, and the individual intrinsic binding affinity of the components of bivalent ligand on the binding properties of bivalent ligands (Figure 2). Representative examples of the effects of these parameters on the affinity of the bivalent ligand are illustrated in Figure 2.

For each of the ligand−target combinations, the full titration experiments with a range of ligand concentrations were performed and the data were analyzed by nonlinear regression analysis to obtain the equilibrium constants describing equilibria depicted in Figure 1C. These constants were then used to calculate the values of c_{eff}. Figure 3A shows the c_{eff} values for different combinations of the individual intrinsic binding affinity constants of the components of the bivalent ligand. The c_{eff} parameter for all combinations of intrinsic binding constants values was very similar (in the range of tenths of micromolar). The lower values of c_{eff} observed for the highest intrinsic affinities of the components of the bivalent ligand (Figure 3A, data for $K_A = 21$ nM and $K_B = 43$ nM) are most likely not significant and reflect the difficulty of fitting the data in this case since the binding of the bivalent ligand was very tight, making biased fitting errors likely. This observed independence of c_{eff} with respect to the intrinsic affinity of individual ligand components indicates that c_{eff} reflects the general properties of the linker and does not depend on specific characteristics of the individual ligands. For each of the intrinsic affinity constant combinations shown in Figure 3B, the c_{eff} also did not change significantly with the length of the linker. All of the data shown in Figure 3A were obtained using the targets with a distance of 6 nm between the binding sites. Apparently, with this shortest distance between the binding sites, even the shortest linker (24 nm) is long enough to allow effective binding of the bivalent ligand.

Figure 3B illustrates the dependence of c_{eff} on the distance between the binding sites of the target. An increased distance between the binding sites resulted in a decrease in c_{eff} [and thus in a decreased affinity of the bivalent ligand (Table S1 of the Supporting Information)]. Bivalent ligands containing low-affinity binders ($K_A = 1.0$ μM, and $K_B = 1.7$ μM) exhibited very little or no enhancement in binding affinity for the target with the longest distance (13 nm) between the binding sites (Table S1 of the Supporting Information). Also, with the longest distance between the sites (13 nm), the dependence of c_{eff} on the linker length became apparent. Bivalent ligands with shorter linkers exhibited reduced c_{eff} values. Overall, the data illustrated in Figure 3 showed that long flexible linkers can be used to create bivalent ligands that could effectively bind to a wide variety of targets differing in distances between the binding sites and their intrinsic binding affinity.

The properties of bivalent ligands under a variety of

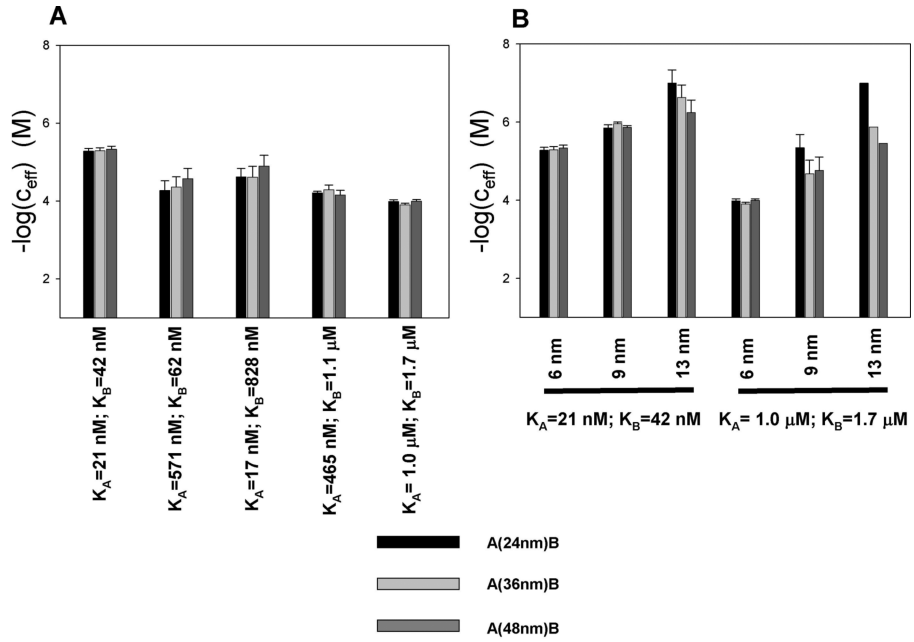

FIGURE 3: (A) Effective concentrations (c_{eff}) determined for various combinations of affinities of individual ligands. For each combination of affinities, c_{eff} was determined for the bivalent ligand with 24 nm [A(24nm)B], 36 nm [A(36nm)B], and 48 nm [A(48nm)B] linker lengths. T(6nm)0, T(6nm)1, T(6nm)2, T(6nm)3, and T(6nm)4 (Table 1) were used as targets. (B) Effect of the distance between the binding sites on the effective concentration (c_{eff}). For each distance between the binding sites, c_{eff} was determined for the bivalent ligand with the 24 nm linker [A(24nm)B], 36 nm linker [A(36nm)B], and 48 nm linker [A(48nm)B]. One series of experiments (first three groups of bars) was performed using T(6nm)0, T(9nm)0, and T(13nm)0 (Table 1) as targets, whereas the second series of experiments (second three groups of bars) was performed using T(6nm)4, T(9nm)4, and T(13nm)4 (Table 1) as targets. The c_{ceff} value for T(13nm)4 and A(24nm)B could not be determined (Table S1 of the Supporting Information), and thus, the value determined for T(13nm)0 and A(24nm)B was plotted as the estimate for this c_{eff}.

conditions can be best illustrated by calculating the relative abundance of various species depicted in Figure 1C. The values of c_{eff}, K_A, and K_B are sufficient to perform these calculations using eqs 5 and 6 and numerical solutions to mass conservation equations derived for the scheme in Figure 1C. Figure 4 summarizes these calculations. Several conclusions are readily apparent upon inspection of Figure 4. The affinity of the bivalent ligand under most of the conditions employed in Figure 4 is greatly enhanced compared to the affinity of the individual ligand components of the bivalent ligand (red vs green curves). As a consequence of that under most conditions, the S5 complex (Figure 1C) in which a bivalent ligand forms a 1:1 complex with the ligand engaging both of the target binding sites is the dominating complex species. Only when the distance between the sites is the longest and the intrinsic affinity of individual ligand components is the weakest (Figure 4C) does linking the two individual ligands with the flexible linker not create a bivalent ligand with improved binding properties. A simple prescription for a bivalent ligand with improved binding properties that can be derived from Figure 4 is that when intrinsic dissociation constants of bivalent ligand components are at least ~10-fold lower than the c_{eff} values, a practically useful bivalent ligand with significantly improved binding affinity will be obtained. The relative degree of affinity enhancement observed for bivalent ligands is proportional to the intrinsic affinity of bivalent ligand components, i.e., the higher the intrinsic affinity of bivalent ligand components, the larger the gain in affinity when they are connected with the flexible linker to form a bivalent ligand. For example, using eq 5 with a c_{eff} of 10 μM [a reasonably typical value for the linkers used in this work (Figure 3)], we can calculate that linking two ligands with intrinsic dissociation constants of 100 nM should produce a bivalent ligand with a dissociation constant of 1 nM (100-fold improved binding affinity). However, linking two ligands with intrinsic dissociation constants of 1 nM should produce a bivalent ligand with a dissociation constant of 0.1 pM (10000-fold improved binding affinity). These numbers can also be used to illustrate the increase in binding specificity that should be observed for bivalent ligands compared to the individual ligand components of the bivalent ligand. One can consider a case of individual ligands that bind the target with a dissociation constant of 1 nM but exhibit an only 100-fold binding specificity (i.e., they bind to nontargets with a dissociation constant of 100 nM). When these ligands are connected with a flexible linker to form a bivalent ligand, its binding specificity will increase 10000-fold as a result of a greater relative increase in affinity for intrinsic dissociation constants of 1 nM compared to intrinsic dissociation constants of 100 nM.

We were interested in seeing how our experimental data with the simple oligonucleotide-based model system compared with the predictions derived from the wormlike chain model developed by Zhou (*16, 17*) for polypeptide linkers. In this model, c_{eff} is calculated from the following expression:

$$p(r) = (3/4\pi l_p l_c)^{3/2} \exp(-3r^2/4l_p l_c)(1 - 5l_p/4l_c + 2r^2/l_c^2 - 33r^4/80l_p l_c^3 - 79l_p^2/160l_c^2 - 329r^2 l_p/120l_c^3 + 6799r^4/1600l_c^4 - 3441r^6/2800l_p l_c^5 + 1089r^8/12800l_p^2 l_c^6) \quad (7)$$

$$c_{eff}\,(\mu M) = p(r) \times 10^{10}/6.022$$

where $p(r)$ is the probability density for the end-to-end vector for the flexible linker to have a distance of r, l_c is the contour

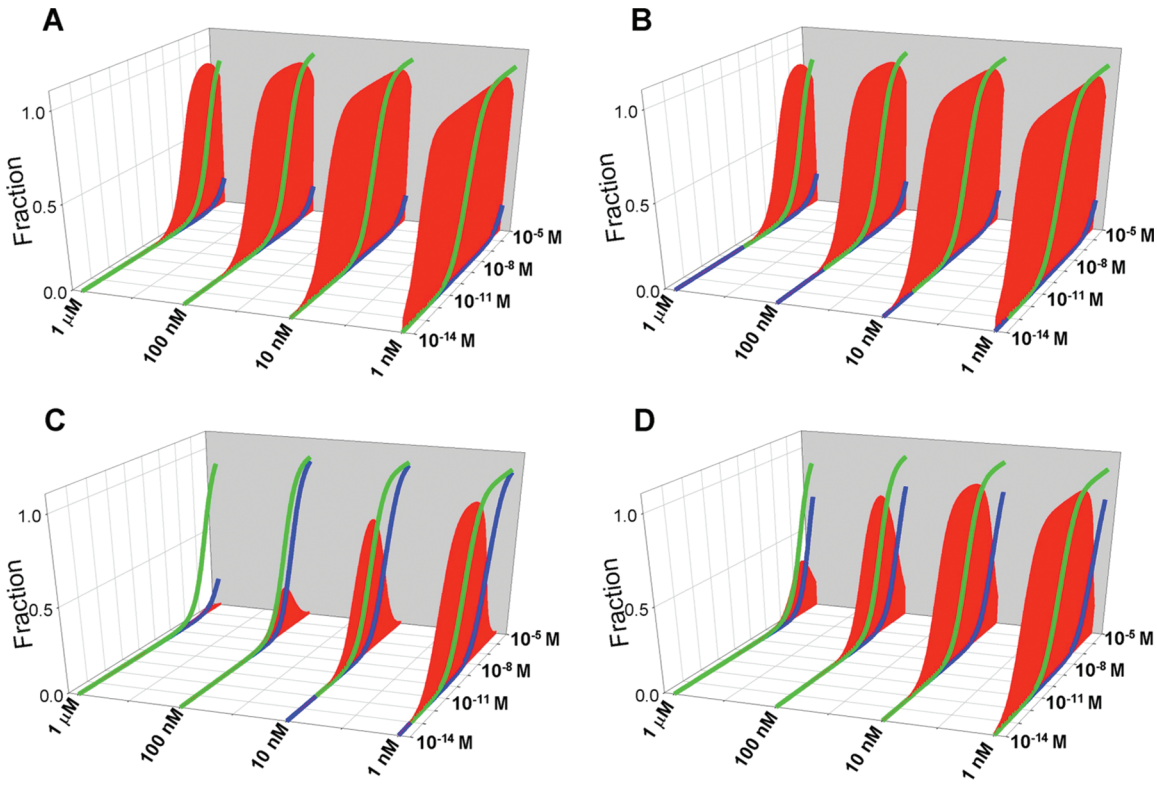

FIGURE 4: Summary of the binding properties of model bivalent ligands. Experimentally determined values of c_{eff} were used to calculate the relative amounts of S5 (red plane) and S6 (blue line) species of the model illustrated in Figure 1C as a function of bivalent ligand concentration (from 10^{-14} to 10^{-5} M). S5 is a binary complex between the target and the bivalent ligand, whereas S6 is a ternary complex containing two bivalent ligands bound to the target. The calculations were conducted for four different affinities of the individual ligand components of the bivalent ligand (affinities for both ligands were set to be the same and corresponded to K_d values of 1 μM, 100 nM, 10 nM, and 1 nM). For the sake of comparison, the saturation curve expected for the individual ligand is shown as well (green line). (A) Calculations corresponding to a 24 nm long ligand binding to a target containing two binding sites separated by 6 nm. (B) Calculations corresponding to a 48 nm long ligand binding to a target containing two binding sites separated by 6 nm. (C) Calculations corresponding to a 24 nm long ligand binding to a target containing two binding sites separated by 13 nm. (D) Calculations corresponding to a 48 nm long ligand binding to a target containing two binding sites separated by 13 nm.

length of the linker, and l_p is the persistence length (0.3 nm in the case of the peptide linker). All of the parameters for calculating c_{eff} for our model bivalent ligands using eq 7 were available with the exception of persistence length (l_p). We performed calculations (Figure 5) of c_{eff} with eq 7 using a range of l_p parameter values and compared them to the experimental data (we used the c_{eff} values determined for the ligands with a low intrinsic affinity of individual bivalent ligand components since, as discussed above, these likely provide the most accurate determination of c_{eff}). Calculations assuming low values of l_p (0.2 or 0.3 nm) were clearly not consistent with the experimental data. The calculated values of c_{eff} were much lower than the experimentally observed values. Also, the very pronounced dependence of c_{eff} on linker length or on the distance between the binding sites apparent in calculated data was not observed experimentally. The best correspondence between the calculated c_{eff} and measured c_{eff} was observed with an l_p value of ~0.5 nm. We had expected a lower persistence length for our PEG-based linkers, on the basis of the persistence length of ~0.3 nm for polypeptide linkers studied by Zhou (*16, 17*). One possible explanation could be that the Spacer18 phosphoramidate that we used to incorporate the PEG linker into our constructs also adds a phosphate group for each addition of the phosphoramidate (thus, for example, the 48 nm linker that required 10 Spacer18 additions contains 10 phosphates). The negative charge introduced by these phosphates could contribute to the increase in the persistence length of the linker. With this persistence length, the calculated and measured values of c_{eff} agreed within ~1 order of magnitude. Also, the experimentally observed lack of change in c_{eff}, a small decrease in c_{eff}, and a significant decrease in c_{eff} with the increase in linker length (from 24 to 48 nm) for 6, 9, and 13 nm spacing between the binding sites, respectively, could be also seen in the c_{eff} predicted using eq 7. Thus, the model represented by eq 7, when used with a persistence length of ~0.5 nm, provides a good first approximation of binding behavior of bivalent ligands connected by very long PEG-based flexible linkers.

In conclusion, the data obtained with model bivalent ligands demonstrated that connecting the ligands with long nanometer-scale flexible linkers is a viable way to produce bivalent ligands with significantly or in some instances greatly enhanced binding affinity and specificity. The nanometer scale and the flexibility of the linker eliminate the need for careful bivalent ligand design since they allow easy adaptation of bivalent ligand conformation to any configuration of binding sites of the target. Furthermore, the nanometer scale of the linker allows the design of bivalent ligands that could exploit target binding sites that are located far from each other.

Enhanced Affinity Bivalent Ligands Targeting Thrombin. In the next step, we sought to verify that the conclusions derived from the simple oligonucleotide-based model (Figure

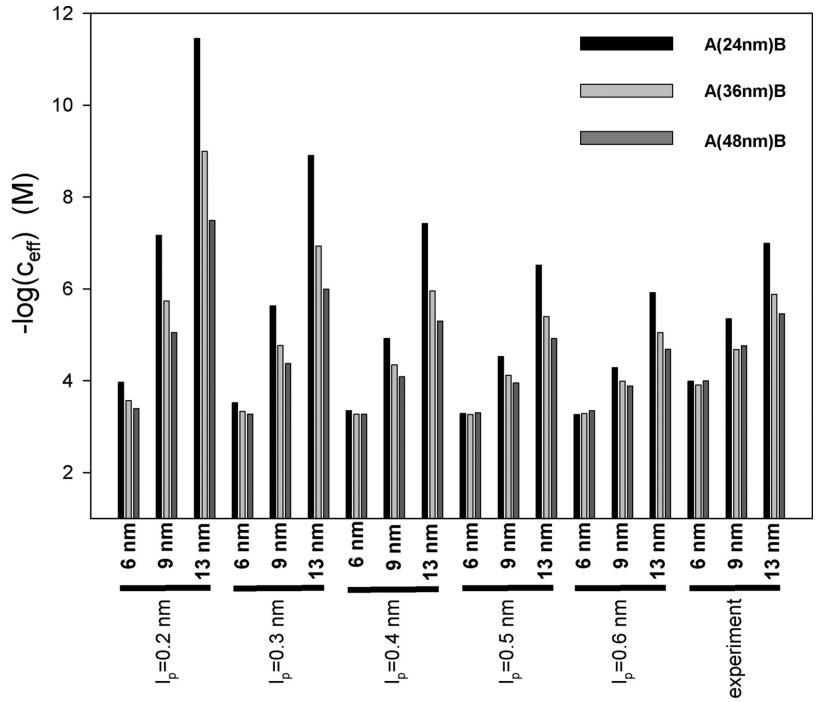

FIGURE 5: Comparison between c_{eff} values predicted by the wormlike chain model and c_{eff} values measured experimentally. The plot shows calculated c_{eff} values (using eq 7) for different values of persistence length (l_p). For the sake of comparison, the last set of bars shows the experimentally determined c_{eff} values.

1) could be indeed used as a guide to prepare an enhanced bivalent ligand for a real biological target. We chose thrombin as a target for bivalent ligand development. Human α-thrombin is a serine protease that plays a key role in blood coagulation. It is generated by the enzymatic cleavage of prothrombin by activated factor X (Xa). Human α-thrombin is a heterodimer consisting of an "A" chain (M_r = 6000) and a "B" chain (M_r = 31000), which are covalently linked to each other through a single disulfide bond. Thrombin converts fibrinogen into fibrin, leading to the formation of the fibrin clot, which is the last step in the blood coagulation pathway (*25*). Thrombin exhibits several other key cellular bioregulatory functions, including the direct activation of protein C and platelet and the feedback activation of the procofactors, factor V and factor VIII (*26, 27*). In addition to the active site, there are two positively charged exosites that mediate the interactions of thrombin with inhibitors and substrates (*25*). Exosite 1 binds fibrinogen, hirudin, thrombomodulin, and heparin cofactor II, while exosite 2 binds heparin, heparan sulfate, glycosaminoglycan, and prothrombin fragment 2. Oligonucleotide-based aptamers G15D and [60−18] 29 have been obtained by in vitro selection from a library of random sequence oligonucleotides. These aptamers selectively bind to exosites 1 and 2 of thrombin (*28, 29*). Several thrombin inhibitors, such as heparin, warfarin, and huridin, have been used clinically to treat thromboembolic disease. Their therapeutic effects are limited because of the narrow therapeutic windows and highly variable dose−response relation among individuals, and the reduced affinity for fibrin-bound thrombin (*30*). New anticoagulants with predictable, stable, and reversible anticoagulation activity are needed. Anti-thrombin aptamers appear to be promising new therapeutics due to their ease of preparation, their low immunogenicity, and their ability to tightly control their anticlotting activities.

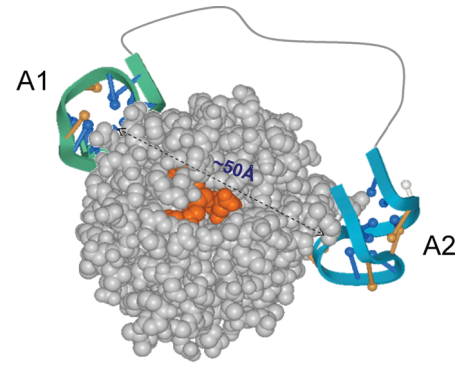

FIGURE 6: Model of the complex between thrombin and the bivalent ligand containing the aptamer binding to exosite 1 (A1) and the aptamer binding to exosite 2 (A2) connected by a long flexible linker.

The thrombin binding sites of G15D (A2) and [60−18] 29 (A1) aptamers are separated by ~5 nm (Figure 6). We designed bivalent ligands in which the two thrombin binding aptamers were connected by 24 nm long linkers (Table 2). The individual aptamers bound thrombin with nanomolar range dissociation constants (Table 3). We used these dissociation constants and c_{eff} values derived from our model bivalent ligand analysis to predict the affinity of bivalent thrombin ligands (Table 3). The predicted affinity constants were calculated using the range of values of c_{eff} (5−100 μM) observed in all model ligand experiments for the ligands containing a 24 nm long linker binding to targets with a distance of 6 nm between the binding sites (the closest match between the model parameters and the thrombin as a target). The affinity of these ligands was then measured in a competition assay employing molecular beacons for thrombin (*21*). As expected, bivalent ligands exhibited greatly enhanced binding affinity (~100-fold) compared to the individual aptamers. However, predicted values of dissociation constants were significantly lower (≥1 order of magnitude)

Table 3: Binding Affinities of Bivalent Thrombin Ligands and Their Components

	A1	A2	biv	A1(12nm)A2	A1(24nm)A2	A2(24nm)A1	biv(24nm)A1
predicted K_d (nM)	−	−	−	0.004−0.002[a]	0.002−0.0001[b]	0.002−0.0001[b]	0.001−0.00005[b]
measured K_d (nM)	2.9	4.0	1.6	0.3	0.06	0.03	0.2

[a] Values calculated with eq 5 using c_{eff} values extrapolated using eq 7 from the experimental data for a 24 nm long linker. [b] The range of the values (calculated with eq 5) shown corresponds to the range of experimentally determined c_{eff} values for the model ligands containing a 24 nm long linker (Figure 3A).

compared to the experimentally observed affinities. This agreement is probably slightly better than that since the experimental values of dissociation constants for A1(24nm)A2 and A2(24nm)A1 should be considered as high estimates for these values because it was very difficult to obtain accurate values for such tight binding ligands using the thrombin molecular beacon assay that was employed (*21*). Nevertheless, these observations suggest that c_{eff} values obtained from experiments with model targets and ligands should be considered as "best scenario" high estimates, and significantly lower values should be expected with real targets of more complex architecture of the binding sites.

We have also made a bivalent ligand with a shorter (12 nm long) linker (Table 3). While we did not directly measure c_{eff} values for this shorter linker using model ligands and targets, eq 7 predicted that the affinity of this ligand should be only ~2-fold lower compared to that of the thrombin ligands with a 24 nm linker. In qualitative agreement with this prediction, the experimentally observed affinity (K_d = 0.3 nM) was 5−10-fold lower compared to those of the ligands containing a 24 nm long linker. The larger difference in the experimentally determined affinity between thrombin ligands containing 24 and 12 nm linkers compared to predictions derived from the model suggests that with shorter linkers differences between a simple model (Figure 1) and a real target with a more complex structure can be more pronounced. The ligands with the same linker lengths [A1(24nm)A2 and A2(24nm)A1] but differing in head-to-head versus head-to-tail configuration of the linked aptamers exhibited significantly different affinities (~2-fold difference), further indicating that binding properties of bivalent ligands can be somewhat affected by steric constraints of more complex targets.

To further explore the generality of flexible linker bivalent ligand design, we constructed a mixed peptide and aptamer-based ligand by linking the A1 aptamer with bivalirudin (Table 2) using a 24 nm long PEG-based flexible linker. Bivalirudin is a synthetic peptide that directly inhibits thrombin by specifically binding to the catalytic site as well as to the anion-binding exosite of circulating and clot-bound thrombin (*31*). Bivaluridin was attached to the linker through a cysteine group (which was added into the poly G region of the bivalirudin peptide). The biv(24nm)A1 (Table 2) bivalent ligand bound to thrombin ~7-fold stronger than bivalirudin or A1 alone. This illustrated that enhanced affinity ligands containing long flexible linkers could be made from heterologous ligands. However, the affinity enhancement observed with this bivalent ligand, while significant, was much smaller compared to those of A1(24nm)A2 and A2(24nm)A1 and was similar to that of the aptamer-based bivalent ligand containing a shorter (12 nm) linker. The likely explanation of this smaller than expected affinity gain is that the attachment of the linker to biv at a site located in a short peptide segment connecting the two segments making a direct contract with thrombin had a negative effect of the affinity of biv for thrombin.

To relate the binding properties of bivalent ligands to their ability to inhibit thrombin activities, we measured their anticlotting activities. Cleavage of fibrinogen to produce the fibrin clot is the primary function of thrombin. The two oligonucleotide-based aptamers, [60−18] 29 (A1) and G15D (A2), selectively bind to exosites II and I on human α-thrombin and thus exhibit their anticlotting activities by directly competing with the substrate fibrinogen or by allostericaly affecting the conformation of active sites. Activated partial thromboplastin time (aPTT) (*23*) measures the efficacy of both the "intrinsic" and "extrinsic" coagulation pathways. We performed the aPTT assays in the presence of bivalent ligand and in the presence of the individual ligand components of the bivalent ligand (Figure 7). The individual aptamers (A1 and A2) exhibited small but significant anticlotting activity (increased clotting time). Bivalent ligands exhibited greatly enhanced anticlotting activities that were correlated with their affinity for thrombin (Figure 7). The bivalent ligand that bound thrombin with the highest affinity exhibited the highest anticlotting activity. Its activity was higher than that of bivaluridin, which is used clinically as an anticoagulant to reduce the risk of acute ischemic complications. The anticlotting activity of biv(24nm)A1 was not improved compared to that of bivaluridin alone. Apparently, either the covalent modification of bivaluridin with the linker had negatively affected bivaluridin activity, or the relatively modest improvement in binding affinity of biv(24nm)A1 compared to that of bivaluridin alone was insufficient to affect its already high anticlotting activity.

One of the advantages of using oligonucleotide-based anticoagulants is that short single-stranded DNA or RNA antidotes that contain sequences complementary to the anticoagulants can control their activities (*7, 32*). Figure 7 shows that the anticlotting activity of bivalent thrombin ligands can be also effectively suppressed with complementary antidote oligonucleotides.

DISCUSSION

Experiments with a simple model showed that as long as the individual binders bound the target with submicromolar affinities, they could be linked by nanometer-scale flexible linkers to produce bivalent ligands with enhanced binding affinity and specificity. Comparison of experimental data with the predictions of a wormlike chain model demonstrated that this model provided a reasonably good description of the binding properties of nanometer-scale flexible bivalent ligands. Experiments with the ligands targeting thrombin showed that the bivalent ligand with improved binding affinity and enhanced biological activity could be obtained for a real biological target. While the data obtained with thrombin ligands were in qualitative agreement with the

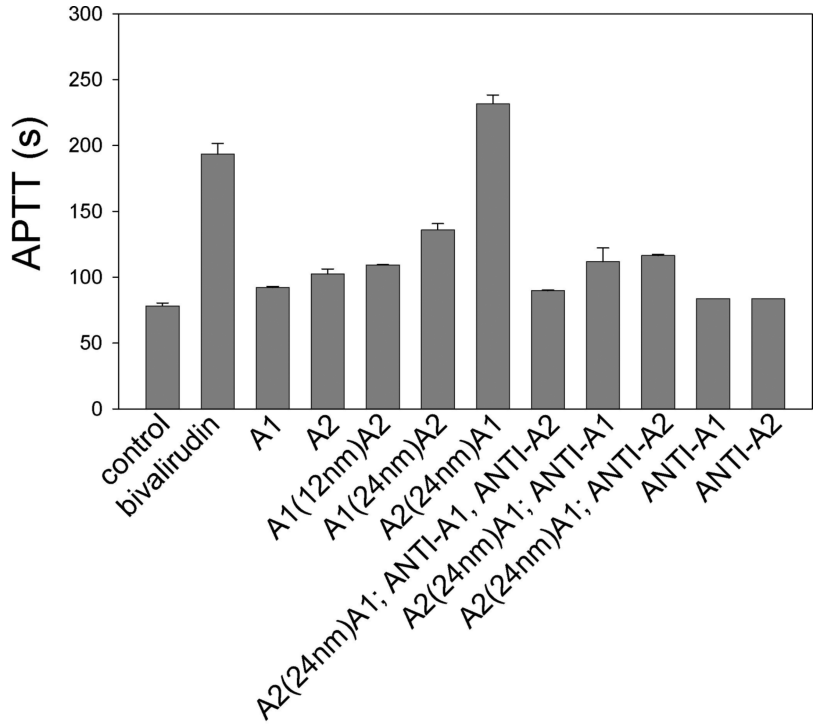

FIGURE 7: Activated partial thromboplastin time (aPTT) in the presence of indicated ligands. aPTT was measured as described in Materials and Methods.

conclusions derived from the model data, the quantitative predictions (based on data obtained with the model system) of the affinity of bivalent ligand for a real target overestimated the experimentally observed affinity by 1−2 orders of magnitude. This difference likely reflects the higher probability of adversely affecting the affinity of individual ligand components of the bivalent ligand for real targets by introducing the cross-linker necessary to connect the ligands. Also, a complex three-dimensional arrangement of binding sites in a real target compared to a simple linear arrangement of binding sites in a DNA-based model is more likely to produce losses in binding energy due to a more limited set of conformations of the linker that will be compatible with simultaneous binding of both components of the bivalent ligand to their respective binding sites.

While this work was being written up, Kim et al. (*33*) reported a very similar design of bivalent aptamer-based inhibitors targeting thrombin. In agreement with the data described here, these authors also observed enhanced anticlotting activity of these constructs. Our data obtained with the model oligonucleotide-based system describe the fundamental principles that explain the observed enhancement of binding affinity and anticlotting activity.

The use of a long flexible linker allows a practical compromise between the ease of preparation of such bivalent ligands and the degree to which their binding properties are improved. While the affinity gain that could be achieved by linking the two binders with long flexible linkers is lower compared to that of a bivalent ligand in which these binders would be held by short rigid linkers in a conformation compatible with their simultaneous binding to the target, it is high enough to be practically useful. A difficult process of assuring that indeed the conformation of the bivalent ligand is compatible with effective interaction with the target is avoided because of the ability of the ligands containing long flexible linkers to adapt to any configuration of the binding sites on the target. The long reach of flexible linkers will allow targeting of the sites of the target that are far from each other, allowing design of bivalent ligands with combinatorial activities not accessible to "normal" binders. While the work described in this paper was focused on oligonucleotide (aptamer)-based ligands, other binders could be utilized as well as long as the chemistry to link them with long flexible linkers exists [as illustrated by an example of a bivaluridin−thrombin aptamer-based bivalent ligand (Table 2)].

ACKNOWLEDGMENT

We thank Dr. Ray Rezaie for the gift of purified human thrombin, and we are very grateful for the invaluable help and assistance of his laboratory in aPTT and thrombin activity measurements.

SUPPORTING INFORMATION AVAILABLE

Table showing a compilation of all experimentally determined dissociation constants and a table showing calculations of the amounts of possible higher-order complexes. This material is available free of charge via the Internet at http://pubs.acs.org.

REFERENCES

1. Hoogenboom, H. R. (2005) Selecting and screening recombinant antibody libraries. *Nat. Biotechnol. 23*, 1105–1116.
2. Lipovsek, D., and Pluckthun, A. (2004) In-vitro protein evolution by ribosome display and mRNA display. *J. Immunol. Methods 290*, 51–67.
3. Nygren, P. A. (2008) Alternative binding proteins: Affibody binding proteins developed from a small three-helix bundle scaffold. *FEBS J. 275*, 2668–2676.
4. Ellington, A. D., and Szostak, J. W. (1990) In vitro selection of RNA molecules that bind specific ligands. *Nature 346*, 818–822.

5. Tuerk, C., and Gold, L. (1990) Systematic evolution of ligands by exponential enrichment: RNA ligands to bacteriophage T4 DNA polymerase. *Science 249*, 505–510.
6. Lee, J. F., Stovall, G. M., and Ellington, A. D. (2006) Aptamer therapeutics advance. *Curr. Opin. Chem. Biol. 10*, 282–289.
7. Yan, A. C., Bell, K. M., Breeden, M. M., and Ellington, A. D. (2005) Aptamers: Prospects in therapeutics and biomedicine. *Front. Biosci. 10*, 1802–1827.
8. Jayasena, S. D. (1999) Aptamers: An emerging class of molecules that rival antibodies in diagnostics. *Clin. Chem. 45*, 1628–1650.
9. Bhushan, R. G., Sharma, S. K., Xie, Z., Daniels, D. J., and Portoghese, P. S. (2004) A bivalent ligand (KDN-21) reveals spinal δ and κ opioid receptors are organized as heterodimers that give rise to δ_1 and κ_2 phenotypes. Selective targeting of $\delta-\kappa$ heterodimers. *J. Med. Chem. 47*, 2969–2972.
10. Paar, J. M., Harris, N. T., Holowka, D., and Baird, B. (2002) Bivalent ligands with rigid double-stranded DNA spacers reveal structural constraints on signaling by FcεRI. *J. Immunol. 169*, 856–864.
11. Portoghese, P. S., Larson, D. L., Sayre, L. M., Yim, C. B., Ronsisvalle, G., Tam, S. W., and Takemori, A. E. (1986) Opioid agonist and antagonist bivalent ligands. The relationship between spacer length and selectivity at multiple opioid receptors. *J. Med. Chem. 29*, 1855–1861.
12. Erez, M., Takemori, A. E., and Portoghese, P. S. (1982) Narcotic antagonistic potency of bivalent ligands which contain β-naltrexamine. Evidence for bridging between proximal recognition sites. *J. Med. Chem. 25*, 847–849.
13. Bergmann, K. E., Wooge, C. H., Carlson, K. E., Katzenellenbogen, B. S., and Katzenellenbogen, J. A. (1994) Bivalent ligands as probes of estrogen receptor action. *J. Steroid Biochem. Mol. Biol. 49*, 139–152.
14. Messer, W. S., Jr. (2004) Bivalent ligands for G protein-coupled receptors. *Curr. Pharm. Des. 10*, 2015–2020.
15. Jencks, W. P. (1981) On the attribution and additivity of binding energies. *Proc. Natl. Acad. Sci. U.S.A. 78*, 4046–4050.
16. Zhou, H. X. (2001) The affinity-enhancing roles of flexible linkers in two-domain DNA-binding proteins. *Biochemistry 40*, 15069–15073.
17. Zhou, H. X. (2003) Quantitative account of the enhanced affinity of two linked scFvs specific for different epitopes on the same antigen. *J. Mol. Biol. 329*, 1–8.
18. Santulli-Marotto, S., Nair, S. K., Rusconi, C., Sullenger, B., and Gilboa, E. (2003) Multivalent RNA aptamers that inhibit CTLA-4 and enhance tumor immunity. *Cancer Res. 63*, 7483–7489.
19. Dollins, C. M., Nair, S., Boczkowski, D., Lee, J., Layzer, J. M., Gilboa, E., and Sullenger, B. A. (2008) Assembling OX40 aptamers on a molecular scaffold to create a receptor-activating aptamer. *Chem. Biol. 15*, 675–682.
20. McNamara, J. O., Kolonias, D., Pastor, F., Mittler, R. S., Chen, L., Giangrande, P. H., Sullenger, B., and Gilboa, E. (2008) Multivalent 4-1BB binding aptamers costimulate CD8+ T cells and inhibit tumor growth in mice. *J. Clin. Invest. 118*, 376–386.
21. Heyduk, E., and Heyduk, T. (2005) Nucleic acid-based fluorescence sensors for detecting proteins. *Anal. Chem. 77*, 1147–1156.
22. Tian, L., and Heyduk, T. (2007) Enhanced affinity bivalent ligands containing long flexible linkers. *2007 Biophysical Society Meeting Abstracts, Biophysical Journal*, Supplement 20a, Abstract, 962-Pos.
23. Langdell, R. D., Wagner, R. H., and Brinkhous, K. M. (1953) Effect of antihemophilic factor on one-stage clotting tests: A presumptive test for hemophilia and a simple one-stage antihemophilic factor assy procedure. *J. Lab. Clin. Med. 41*, 637–647.
24. Crothers, D. M., and Metzger, H. (1972) The influence of polyvalency on the binding properties of antibodies. *Immunochemistry 9*, 341–357.
25. Tullinsky, A. (1996) Molecular interactions of thrombin. *Semin. Thromb. Haemostasis 22*, 117–124.
26. Brummel, K. E., Paradis, S. G., Butenas, S., and Mann, K. G. (2002) Thrombin functions during tissue factor-induced blood coagulation. *Blood 100*, 148–152.
27. Coughlin, S. R. (2000) Thrombin signalling and protease-activated receptors. *Nature 407*, 258–264.
28. Bock, L. C., Griffin, L. C., Latham, J. A., Vermaas, E. H., and Toole, J. J. (1992) Selection of single-stranded DNA molecules that bind and inhibit human thrombin. *Nature 355*, 564–566.
29. Tasset, D. M., Kubik, M. F., and Steiner, W. (1997) Oligonucleotide inhibitors of human thrombin that bind distinct epitopes. *J. Mol. Biol. 272*, 688–698.
30. Weitz, J. I., Hudoba, M., Massel, D., Maraganore, J., and Hirsh, J. (1990) Clot-bound thrombin is protected from inhibition by heparin-antithrombin III but is susceptible to inactivation by antithrombin III-independent inhibitors. *J. Clin. Invest. 86*, 385–391.
31. Maraganore, J. M., Bourdon, P., Jablonski, J., Ramachandran, K. L., and Fenton, J. W., II (1990) Design and characterization of hirulogs: A novel class of bivalent peptide inhibitors of thrombin. *Biochemistry 29*, 7095–7101.
32. Rusconi, C. P., Roberts, J. D., Pitoc, G. A., Nimjee, S. M., White, R. R., Quick, G., Jr., Scardino, E., Fay, W. P., and Sullenger, B. A. (2004) Antidote-mediated control of an anticoagulant aptamer in vivo. *Nat. Biotechnol. 22*, 1423–1428.
33. Kim, Y., Cao, Z., and Tan, W. (2008) Molecular assembly for high-performance bivalent nucleic acid inhibitor. *Proc. Natl. Acad. Sci. U.S.A. 105*, 5664–5669.

BI801630B